A Multiphase Dual-Inverter Supplied Drive Structure for Electric and Hybrid Electric Vehicles(IEEEVPPC2010)

by Metta Savitri

Submission date: 16-Apr-2023 07:05AM (UTC-0500)
Submission ID: 2065820611
File name: ture_for_Electric_and_Hybrid_Electric_Vehicles_IEEEVPPC2010.pdf (702.01K)
Word count: 5952
Character count: 27776

A Multiphase Dual-Inverter Supplied Drive Structure for Electric and Hybrid Electric Vehicles

Emil Levi, Martin Jones, Wahyu Satiawan
Liverpool John Moores University, School of Engineering
Liverpool L3 3AF, United Kingdom
e.levi@ljmu.ac.uk m.jones2@ljmu.ac.uk i.n.satiawan@2008.ljmu.ac.uk

***Abstract*–Open-end winding variable speed drives with dual-inverter supply have been extensively investigated for various applications, including series hybrid powertrains and propulsion motors. The existing body of work is restricted to the three-phase electric machinery. This paper looks at the possibility of using machines with higher phase numbers in an open-end winding configuration with dual multiphase inverter supply for these applications. Switching states for various phase numbers are considered first. Next, a study of the existing space vectors in a five-phase dual-inverter drive configuration is undertaken. This is followed by the discussion of the possible approaches to PWM control of such a drive system. Some simulation results for one particular PWM technique are finally reported.**

I. INTRODUCTION

One particular configuration of a variable-speed drive, consisting of an open-end structure of the stator winding that is supplied from both ends with a voltage source inverter (VSI), has been under scrutiny for three-phase machines recently [1,2]. Typically, two two-level three-phase VSIs are utilised. Application of such a dual-inverter supply enables drive operation with voltage waveform equivalent to the one obtainable with a three-level VSI in single-sided supply mode. Three-phase open-end winding dual-inverter fed drive systems are currently considered as possible alternative supply solutions in EVs/HEVs [3-6], for electric ship propulsion [7], rolling mills [8], etc. The perceived advantages with respect to the equivalent multi-level single-sided supply are the following:

i) The drive availability is improved since in case of a failure of one inverter, it can be shut down and operation resumed with the remaining healthy inverter in single-sided supply mode.
ii) In applications such as EVs, where dc bus voltage is rather low and limited, a machine with a lower current rating can be utilised since the voltage across phases can be higher when two independent batteries are used instead of a single one [3,6].
iii) Assuming that both inverters are two-level, the number of the switches is the same as in the equivalent three-level single-sided supply. However, additional diodes used in the diode-clamped (NPC) VSI are not needed, leading to a saving in the overall number of components. The problem of capacitor voltage balancing does not exist if the supply is two-level at each winding side.

The two VSIs, applied at the two sides of the three-phase open-end winding, can be of the same or of a different number of levels. Use of two two-level VSIs is the most frequently analysed case. Analyses of the system with two three-level inverters are reported in [1,7,9], while use of a combination of a two-level and a three-level VSI has been considered in [8]. Topologies based on the inverters with higher number of levels have also been investigated, e.g. [10].

Multiphase (more than three stator phases) variable-speed drive and generation systems are currently regarded as another type of potentially viable solutions for the same applications, including EVs/HEVs [11]. A two-level multiphase VSI is the standard solution, with the star-connected machine winding and an isolated neutral point. Since multi-level and multiphase topologies share a number of common features, it appears to be logical to try to combine them by realising multi-level multiphase drive architectures. Yet, such attempts are rather rare, with very few examples [12,13], all related to the single-sided supply mode.

A multiphase drive system in an open-end winding configuration has been considered in [14], where an asymmetrical six-phase induction motor drive has been analysed. Two isolated dc voltage supplies were used as the inverter inputs at two winding ends. The goal in [14] was in essence low-order harmonic elimination/reduction rather than the multi-level operation. Hence multi-level operation was neither attempted nor achieved and the drive was operated in all regimes with the voltage waveform equivalent to two-level VSI supply in single-sided mode.

On the basis of the provided survey, it follows that multi-level multiphase supply in open-end winding configuration has never been either addressed or realised. This paper therefore represents the first attempt in this direction. General properties of such a supply configuration are at first discussed, with emphasis placed on the odd phase numbers. A detailed study of the available switching states and corresponding voltage space vectors is conducted next for a five-phase open-end winding drive. Finally, approaches to PWM are discussed and some preliminary simulation results are provided for one possible PWM scheme.

The electric machine/power electronic supply topology, analysed in the paper, is believed to be well suited to two different architectures encountered in EVs and HEVs, respectively. In the case of an electric vehicle, the dual-inverter supply is applicable in conjunction with the propulsion motor(s). Two separate batteries can be used as the inverter supply sources, thus effectively enabling utilisation of a motor with a higher voltage (and hence lower current) rating, compared to the single-battery, single-sided supply mode. In a HEV this topology can be used in

conjunction with the generator, as a part of the series hybrid powertrain [4,5].

II. General Considerations

General topology of a multiphase open-end winding electric machine with a dual-inverter supply is shown in Fig. 1. The number of stator phases n is considered to be odd, while the two VSIs can be of the same or of a different number of levels, m and j, respectively. Two dc sources V_{dc1} and V_{dc2} can be the same source, which reduces the structure to single-phase H-bridge supply of each phase [15], yields only three levels for phase voltages, and causes problems in relation to the zero sequence current [1,2]. Alternatively, two isolated dc sources can be used, in which case zero-sequence current cannot flow and the number of levels in phase voltage can be substantially increased. This case is considered in this paper. When isolated sources are used, there are various possibilities for selection of the ratio of the dc voltages.

The total number of the switching states of such a dual-inverter topology is governed by the number of phases and the numbers of levels of two inverters, according to the law $m^n \cdot j^n$. Table I illustrates the total number of switching states for various phase numbers and a couple of levels of the inverters (it is assumed that $m=j$ for simplicity). Total number of available voltage space vectors for the dual-inverter system of Fig. 1 cannot be determined unless the correlation between the two dc source voltages is given. However, as the number of levels increases, there will be more and more redundant switching states. If single-sided multi-level VSI supply is used, than the corresponding numbers of switching states and voltage space vectors are as shown in Table II [16].

TABLE I. NUMBER OF SWITCHING STATES FOR THE TOPOLOGY OF FIG. 1 AS A FUNCTION OF THE PHASE AND LEVEL NUMBERS.

$m=j$ | n	3	5	7
2	64	1024	16,384
3	729	59,049	4,782,969
5	15,625	9,765,625	6,103,515,625

TABLE II. NUMBER OF SWITCHING STATES AND VOLTAGE SPACE VECTORS (IN BRACKETS) IN SINGLE-SIDED MULTI-LEVEL MULTIPHASE SUPPLY CONFIGURATION [15].

m | n	3	5	7
2	8 (7)	32 (31)	128 (127)
3	27 (19)	243 (211)	2,187 (2,059)
5	125 (61)	3,125 (2,101)	78,125 (61,741)

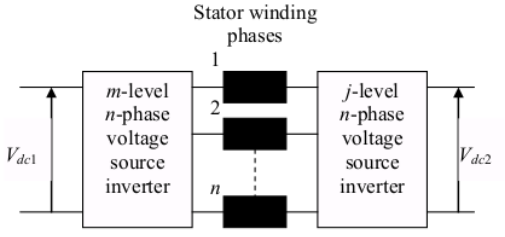

Fig. 1. Dual-inverter supply of an n-phase open-end winding machine.

It can be seen from Table II that an increase in the number of phases dramatically increases the number of switching states, the number of space vectors, and the number of redundant switching states, when compared to the three-phase case (the first column). Using two-level VSIs in dual-inverter supply mode corresponds, in terms of the number of phase voltage levels, to three-level VSI in single-sided supply mode. Similarly, using three-level VSIs in dual-inverter case corresponds to the five-level VSI in single-sided mode, etc. By comparing the relevant rows in Tables I and II, it can be easily concluded that the dual-inverter supply leads to a further exponential increase in the number of switching states, compared to the corresponding single-sided supply for the given phase number. Considering that the supply modulation law needs to be designed by at first selecting the appropriate voltage space vectors for the given reference, and then selecting the most appropriate switching states that will generate selected space vectors while trying to equalise the switching frequency of the switches within a VSI, it is obvious that the dual-inverter multiphase multi-level VSI supply solution presents a considerable challenge.

A further difficulty in realisation of the dual-inverter space vector PWM is associated with the properties of multiphase systems in general. A three-phase system with single-sided supply and isolated neutral point reduces to a two-dimensional (2D) problem, so that space vector PWM can be designed by considering voltage space vectors and switching states in a single plane. In the open-end winding configuration a three-phase system becomes a 3D problem, which is still relatively simple to handle. However, an n-phase system (n = odd number) in single-sided mode of supply is an (n–1)-dimensional problem [11], while in the open-end winding configuration it becomes n-dimensional. An (n–1)-dimensional space can be decomposed into (n–1)/2 mutually perpendicular and hence decoupled 2D sub-spaces [11] and various low-order supply harmonics map into different 2D sub-spaces according to the well-known rules [11]. Any multiphase machine with near-sinusoidal magneto-motive force distribution presents extremely low impedance to all non-flux/torque producing supply harmonics and it is therefore mandatory that the supply does not generate such harmonics. What this means is that the design of any multiphase PWM strategy must consider simultaneously all (n–1)/2 2D sub-spaces, where the reference voltage, assuming pure sinusoidal references, is in the first plane while references in all the other planes are zero. Such space vector PWM strategies have so far been successfully designed only for single-sided supply mode using two-level VSIs, e.g. [17,18], and multi-level multiphase VSIs [12,13]. No attempt has ever been made to design a space vector multi-level multiphase PWM strategy for the dual-inverter open-end configuration of Fig. 1.

Consider an n-phase system. It can be decomposed into (n-1)/2 2D mutually perpendicular planes and a single-dimensional zero-sequence (n = odd). Let the first plane be denoted with indices α–β, while all the other planes are labelled as x-y with an additional numerical index 1, 2…(n-3)/2. Space vector PWM requires application of n voltage

space vectors in a switching period T_s [17,18]. In the case of single-sided two-level VSI supply this comes down to four active space vectors and a zero vector. In the case of multi-level supply, n space vectors are again required, but zero vector is not necessarily involved. Assuming that the set of n space vectors has been somehow selected, the application times of the n vectors are governed with reference voltages in the (n-1)/2 2D planes according to:

$$\begin{aligned}
&\sum_{k=1}^{n} v_{k\alpha}\cdot t_k = v_\alpha^* T_s && \sum_{k=1}^{n} v_{k\beta}\cdot t_k = v_\beta^* T_s \\
&\sum_{k=1}^{n} v_{kx1}\cdot t_k = v_{x1}^* T_s && \sum_{k=1}^{n} v_{ky1}\cdot t_k = v_{y1}^* T_s \\
&\sum_{k=1}^{n} v_{kx2}\cdot t_k = v_{x2}^* T_s && \sum_{k=1}^{n} v_{ky2}\cdot t_k = v_{y2}^* T_s \\
&\text{----------} && \\
&\sum_{k=1}^{n} v_{kx(n-3)/2}\cdot t_k = v_{x(n-3)/2}^* T_s && \sum_{k=1}^{n} v_{ky(n-3)/2}\cdot t_k = v_{y(n-3)/2}^* T_s \\
&\sum_{k=1}^{n} t_k = T_s &&
\end{aligned} \tag{1}$$

Here symbol * identifies references. For a machine with sinusoidal mmf distribution, reference voltages exist only in α–β plane, so that all x-y voltage references in (1) are zero.

It follows from (1) and the previous discussion that, provided that the required n space vectors have been somehow selected, the realisation of the space vector PWM will be straightforward. Hence the first step towards realisation of a space vector PWM strategy is determination of the phase voltage space vectors. A detailed analysis of the switching states and space vectors is therefore performed next for the five-phase open-end winding structure.

III. Five-Phase Open-End Winding Configuration

Fig. 2 illustrates the structure based on utilisation of two two-level five-phase VSIs. The two inverters are identified with indices 1 and 2. Inverter legs are denoted with capital letters, A,B,C,D,E and the negative rails of the two dc links are identified as $N1$ and $N2$. Machine phases are labelled as a,b,c,d,e. Phase voltage positive direction is with reference to the left inverter (inverter 1). Using the notation of Fig. 2, phase voltages of the stator winding can be given as:

$$\begin{aligned}
v_a &= v_{A1N1} + v_{N1N2} - v_{A2N2} \\
v_b &= v_{B1N1} + v_{N1N2} - v_{B2N2} \\
v_c &= v_{C1N1} + v_{N1N2} - v_{C2N2} \\
v_d &= v_{D1N1} + v_{N1N2} - v_{D2N2} \\
v_e &= v_{E1N1} + v_{N1N2} - v_{E2N2}
\end{aligned} \tag{2}$$

Since two isolated dc supplies are assumed further on, the common mode voltage v_{N1N2} is of non-zero value. The issue of CMV elimination is not addressed here.

Space vectors of a five-phase system are defined as [11]

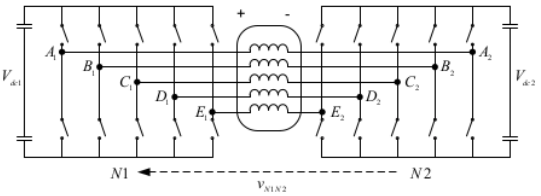

Fig. 2. Five-phase machine with dual two-level inverter supply.

$$\begin{aligned}
\underline{v}_{\alpha-\beta} &= (2/5)\left(v_a + \underline{a}v_b + \underline{a}^2 v_c + \underline{a}^3 v_d + \underline{a}^4 v_e\right) \\
\underline{v}_{x-y} &= (2/5)\left(v_a + \underline{a}^2 v_b + \underline{a}^4 v_c + \underline{a}^6 v_d + \underline{a}^8 v_e\right)
\end{aligned} \tag{3}$$

where $\underline{a} = \exp(j2\pi/5)$ The resulting vectors in dual-inverter supply mode will depend on the ratio of the two dc bus voltages. The situation considered further on is the setting $V_{dc1} = V_{dc2} = V_{dc}/2$, which gives the equivalent of single-sided three-level supply. In a three-phase case this gives nine levels in the phase voltages (including +/- values and zero). Since in five-phase case single-sided supply gives nine levels in the phase voltages, it is then expected that in five-phase case with dual-inverter supply there will be up to 17 levels in the phase voltage. Here V_{dc} stands for the equivalent dc voltage in single-sided supply mode.

Using (2) and (3), space vectors of phase voltages are

$$\begin{aligned}
\underline{v}_{\alpha-\beta} &= \underline{v}_{\alpha-\beta(A1B1C1D1E1)} - \underline{v}_{\alpha-\beta(A2B2C2D2E2)} \\
\underline{v}_{x-y} &= \underline{v}_{x-y(A1B1C1D1E1)} - \underline{v}_{x-y(A2B2C2D2E2)}
\end{aligned} \tag{4}$$

since $v_{N1N2}(1+\underline{a}+\underline{a}^2+\underline{a}^3+\underline{a}^4) = 0$. In (4) the two space vectors on the right-hand sides of the two equations are corresponding voltage space vectors of the two five-phase two-level VSIs.

Space vectors of the five-phase inverter, in the first plane, are as shown in Table III. Corresponding vectors in the second plane are shown in Table IV. There are three vector lengths, large, medium and small: $0.4(0.5V_{dc})2\cos(\pi/5)$, $0.4(0.5V_{dc})$, $0.4(0.5V_{dc})2\cos(2\pi/5)$. Vector lengths are for simplicity denoted further on as:

$$\begin{aligned}
\Gamma &= 0.4(0.5V_{dc})2\cos(\pi/5) = 0.3236V_{dc} \\
\Delta &= 0.4(0.5V_{dc}) = 0.2V_{dc} \\
\Lambda &= 0.4(0.5V_{dc})2\cos(2\pi/5) = 0.1236V_{dc}
\end{aligned} \tag{5}$$

and splitting of the total dc voltage into equal parts is accounted for in (5) (i.e. $V_{dc1} = V_{dc2} = V_{dc}/2$). Voltage space vectors, produced by the 1024 possible switching states, are studied next.

IV. Phase Voltage Space Vectors

In what follows only the first plane is considered. Similar considerations and an identical method of analysis apply to the second plane. The derivations are based on the first of (4),

$$\underline{v}_{\alpha-\beta} = \underline{v}_{\alpha-\beta(A1B1C1D1E1)} - \underline{v}_{\alpha-\beta(A2B2C2D2E2)} \tag{6}$$

where the space vectors at the two sides of the machine can be any out of the 31 listed in Table III (with two switching states defining one zero space vector).

Using (5) and (6), phase voltage space vectors in the α–β plane can be expressed in a generic form as

$$\underline{v}_{\alpha-\beta} = A\exp(jk\pi/5) - B\exp(jl\pi/5) \quad (7)$$

where $A \in \{0, \Gamma, \Delta, \Lambda\}$, $B \in \{0, \Gamma, \Delta, \Lambda\}$, $k = 0,1,2\ldots9$, and, finally, $l = 0,1,2\ldots9$. Coefficients Γ, Δ and Λ are in what follows normalised with respect to the dc voltage V_{dc}.

A. Switching states giving zero phase voltage space vector

A switching state will result in the zero space vector in the following two cases: $A = B = 0$ (four states), $A = B \in \{\Gamma, \Delta, \Lambda\}$ with $k = l$ (thirty states). Hence there are a total of 34 switching states leading to the zero space vector.

B. Switching states yielding the equivalent of single-sided two-level operation with non-zero voltage space vector

In this mode one of the two inverters is kept in zero switching state, while the other may operate with any of the 30 active space vectors. Hence there are 30 states to consider, from each inverter side, and for two possible zero switching states of the other inverter. This is a total of 120 (30x4) switching states, with 30 non-zero active vectors. The vectors form three sets, each with ten active space vectors, and there are four switching states per vector. The vector lengths are:

$$\underline{v}_{\alpha-\beta} = \Gamma\exp(jk\pi/5)$$
$$\underline{v}_{\alpha-\beta} = \Delta\exp(jk\pi/5), \quad k = 0,1,2,\ldots,9 \quad (8)$$
$$\underline{v}_{\alpha-\beta} = \Lambda\exp(jk\pi/5)$$

C. Switching states due to equal vector application at the two winding sides

This section considers the situation that arises when $A = B$ and $k = 0,1,2\ldots9$, $l = 0,1,2\ldots9$, with the condition that $k \neq l$:

$$\underline{v}_{\alpha-\beta} = A[\exp(jk\pi/5) - \exp(jl\pi/5)];\ k,l = 0,1\ldots9,\ k \neq l \quad (9)$$

The results are summarised in Tables V, VI and VII for large-large, medium-medium and small-small vectors, respectively.

TABLE III. PHASE VOLTAGE SPACE VECTORS OF A FIVE-PHASE VSI IN THE FIRST (α–β) PLANE [20].

Space vectors	Value of the space vectors
$\underline{v}_1$ to $\underline{v}_{10}$ (large)	$0.4(0.5V_{dc})2\cos(\pi/5)\exp(jk\pi/5)$ $k = 0,1,2\ldots.9$
$\underline{v}_{11}$ to $\underline{v}_{20}$ (medium)	$0.4(0.5V_{dc})\exp(jk\pi/5)$ $k = 0,1,2\ldots.9$
$\underline{v}_{21}$ to $\underline{v}_{30}$ (small)	$0.4(0.5V_{dc})2\cos(2\pi/5)\exp(jk\pi/5)$ $k = 0,1,2\ldots.9$
$\underline{v}_{31}$ to $\underline{v}_{32}$	0

TABLE IV. PHASE VOLTAGE SPACE VECTORS OF A FIVE-PHASE VSI IN THE SECOND (x-y) PLANE.

Space vectors	Value of the space vectors
$\underline{v}_{21}$ to $\underline{v}_{30}$	$0.4(0.5V_{dc})2\cos(\pi/5)\exp(jk\pi/5)$ $k = 0,1,2\ldots.9$
$\underline{v}_{11}$ to $\underline{v}_{20}$	$0.4(0.5V_{dc})\exp(jk\pi/5)$ $k = 0,1,2\ldots.9$
$\underline{v}_1$ to $\underline{v}_{10}$	$0.4(0.5V_{dc})2\cos(2\pi/5)\exp(jk\pi/5)$ $k = 0,1,2\ldots.9$
$\underline{v}_{31}$ to $\underline{v}_{32}$	0

TABLE V. SPACE VECTORS PRODUCED BY THE INTERACTION OF LARGE-LARGE VECTORS AT THE TWO WINDING SIDES.

$V_{dc1} = V_{dc2} = 0.5V_{dc}$	l	Angular positions
0.6472	k+5	$k\pi/5$
0.2	k+1	$(k-2)\pi/5$
	k+9	$(k+2)\pi/5$
0.3804	k+2	$(2k-3)\pi/10$
	k+8	$(2k+3)\pi/10$
0.5236	k+3	$(k-1)\pi/5$
	k+7	$(k+1)\pi/5$
0.6155	k+4	$(2k-1)\pi/10$
	k+6	$(2k+1)\pi/10$

TABLE VI. SPACE VECTORS PRODUCED BY THE INTERACTION OF MEDIUM-MEDIUM VECTORS AT THE TWO WINDING SIDES.

$V_{dc1} = V_{dc2} = 0.5V_{dc}$	l	Angular positions
0.4	k+5	$k\pi/5$
0.1236	k+1	$(k-2)\pi/5$
	k+9	$(k+2)\pi/5$
0.23451	k+2	$(2k-3)\pi/10$
	k+8	$(2k+3)\pi/10$
0.3236	k+3	$(k-1)\pi/5$
	k+7	$(k+1)\pi/5$
0.3804	k+4	$(2k-1)\pi/10$
	k+6	$(2k+1)\pi/10$

TABLE VII. SPACE VECTORS PRODUCED BY THE INTERACTION OF SMALL-SMALL VECTORS AT THE TWO WINDING SIDES.

$V_{dc1} = V_{dc2} = 0.5V_{dc}$	l	Angular positions
0.2472	k+5	$k\pi/5$
0.0764	k+1	$(k-2)\pi/5$
	k+9	$(k+2)\pi/5$
0.1453	k+2	$(2k-3)\pi/10$
	k+8	$(2k+3)\pi/10$
0.2	k+3	$(k-1)\pi/5$
	k+7	$(k+1)\pi/5$
0.2351	k+4	$(2k-1)\pi/10$
	k+6	$(2k+1)\pi/10$

Each combination yields 90 switching states that yield non-zero space vectors. In each of the three tables k =0,1,2…9 applies and per-unit values are given. Hence 270 switching states are covered by Tables V-VII. Vector lengths in bold in Tables V-VII identify new sets of space vectors that have not been encountered in the previous sub-section or in previous table(s). Hence Tables V-VII define 40+20+30=90 unique space vectors, obtainable in 270 switching states.

D. Switching states due to unequal vector application at the two winding sides

Combination of large-medium active space vectors yields the results given in Table VIII. The same vectors result with medium-large combination. Hence Table VIII covers 200 switching states and yields a total of 40 new space vectors, not found so far. Similarly, 200 switching states associated with large-small and small-large vector application lead to the vectors summarised in Table IX. There are 30 new space vectors in Table IX. Finally, space vectors produced by the

interaction of medium-small and small-medium vectors are summarised in Table X. These 200 switching states lead to 20 space vectors that have not been encountered before.

Note that the angular positions in Tables VII-X are only apparently different, since $k\pi/5 - 26.27° = (k\text{-}1)\pi/5 + 9.73°$, $k\pi/5 - 13.61° = (k\text{-}1)\pi/5 + 22.386°$, etc.

Summarising the results of Tables V-X and the analysis, it follows that the total number of voltage space vectors in five-phase dual two-level VSI configuration is 211. In addition to the zero vector, there are 210 active space vectors. This is exactly the same as in the case of a five-phase three-level supply in single-sided mode, Table II. However, these vectors can be achieved with 1024 switching state combinations, which is significantly more than with a single three-level VSI (only 243 states).

TABLE VIII. SPACE VECTORS PRODUCED BY THE INTERACTION OF LARGE-MEDIUM VECTORS AT THE TWO WINDING SIDES.

$V_{dc1} = V_{dc2} = 0.5V_{dc}$	l	Angular position
0.5236	k+5	$k\pi/5$
0.2	k+1	$k\pi/5$
0.3236	k+2	$k\pi/5$
0.4298	k+3	$k\pi/5 - 26.27°$
0.4994	k+4	$k\pi/5 - 13.614°$
0.4994	k+6	$k\pi/5 + 13.614°$
0.4298	k+7	$k\pi/5 + 26.27°$
0.3236	k+8	$k\pi/5$
0.2	k+9	$k\pi/5$
0.1236	k	$k\pi/5$

TABLE IX. SPACE VECTORS PRODUCED BY THE INTERACTION OF LARGE-SMALL VECTORS AT THE TWO WINDING SIDES.

$V_{dc1} = V_{dc2} = 0.5V_{dc}$	l	Position
0.4472	k+5	$k\pi/5$
0.2351	k+1	$(2k\text{-}1)\pi/10$
0.30865	k+2	$k\pi/5 - 22.386°$
0.3804	k+3	$(2k\text{-}1)\pi/10°$
0.4298	k+4	$k\pi/5 - 9.73°$
0.4298	k+6	$k\pi/5 + 9.73°$
0.3804	k+7	$(2k\text{-}1)\pi/10$
0.30865	k+8	$k\pi/5 + 22.386°$
0.2351	k+9	$(2k\text{+}1)\pi/10$
0.2	k	$k\pi/5$

TABLE X. SPACE VECTORS PRODUCED BY THE INTERACTION OF MEDIUM-SMALL VECTORS AT THE TWO WINDING SIDES.

$V_{dc1} = V_{dc2} = 0.5\ V_{dc}$	l	Position
0.3236	k+5	$k\pi/5$
0.1236	k+1	$k\pi/5$
0.2	k+2	$k\pi/5$
0.2656	k+3	$k\pi/5 - 26.26°$
0.3085	k+4	$k\pi/5 - 13.61°$
0.3805	k+6	$k\pi/5 + 13.61°$
0.2656	k+7	$k\pi/5 + 26.26°$
0.2	k+8	$k\pi/5$
0.1236	k+9	$k\pi/5$
0.0764	k	$k\pi/5$

E. Graphical representation

Distribution of all 211 phase voltage space vectors in α–β and x-y planes is depicted in Fig. 3. A zoomed extract for the first sector only is shown in Fig. 4. As can be seen, there are nine vector groups of different lengths at positions $k\pi/5$, four vector groups at positions $(2k\pm3)\pi/10$, and four groups, with two vector lengths each, at angular positions governed with Tables VIII-X that are not multiples of 18 degrees. This constitutes a total of 21 active phase voltage space vectors per 36 degrees sector.

Space vector mapping into the two planes follows the pattern that exists for a five-phase VSI, Tables III and IV. The largest vectors of the first plane map into the smallest vectors of the second plane, and vice versa.

For the reasons detailed in the next section, of particular interest are the space vectors that result due to interaction of large-large, large-medium and medium-medium active space vectors at the two winding sides. Hence Fig. 5 illustrates this particular sub-set of the total space vector set. A total of 130 active space vectors exist in this sub-set.

V. POSSIBLE APPROACHES TO SPACE VECTOR PWM

In principle, it should be possible to realise a space vector PWM scheme based on the complete set of active space vectors of Fig. 3. The principle problem is the selection of the active space vectors, where there is a total of 21 space vectors at disposal in each 36 degrees sector. Hence a more prudent approach appears to be independent control of two five-phase

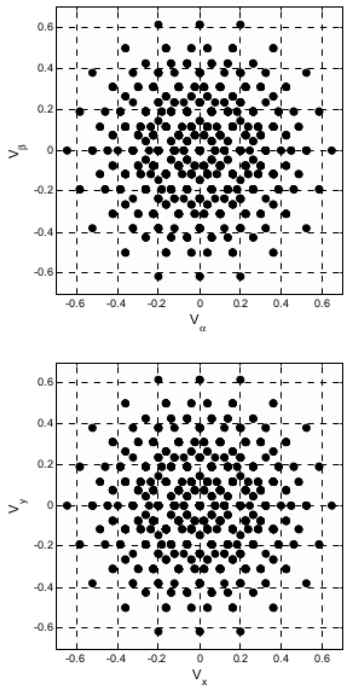

Fig. 3. Space vector distribution in the α–β and x-y planes.

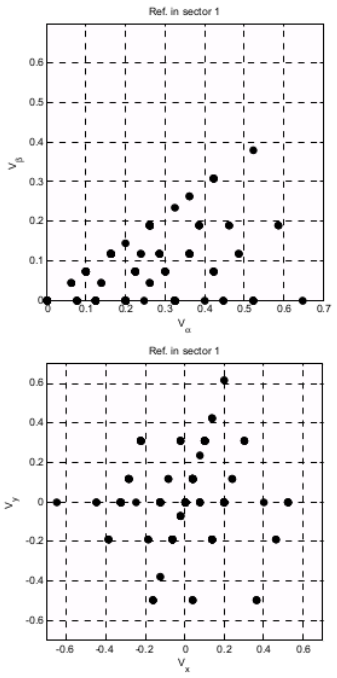

Fig. 4. Space vectors in the first sector of α–β plane and their mapping into the x-y plane.

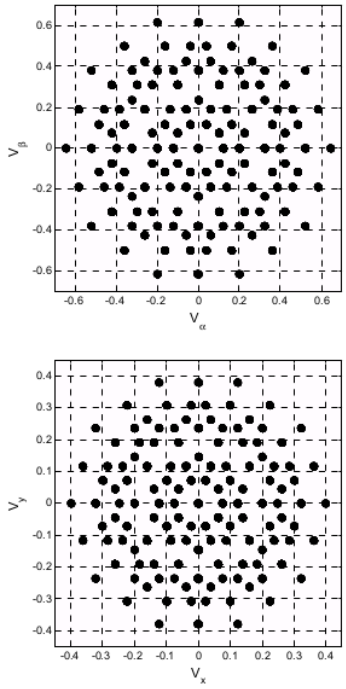

Fig. 5. Phase voltage space vectors in two planes, produced by large-large, medium-medium and large-medium vectors at the two winding sides.

VSIs, since this simplifies considerably the problem of the active vector selection. Since the goal is to realise the reference in the first plane, while keeping the average voltage in the second plane at zero in each switching period, then one needs to apply only four large and medium length space vectors from each five-phase VSI [17]. This is the reason why this sub-set has been already illustrated in Fig. 5. Such an approach reduces the total number of active space vectors that have to be considered from 210 to 130. It also simultaneously ensures that the activated vectors in the second plane, where the reference is zero, are of considerably smaller value than in the first plane. However, if the two inverters are operated independently (albeit at the same switching frequency), it is necessary to split somehow the reference voltage of the α–β plane into two voltage references, one per inverter.

The simplest and rather obvious choice is to split the reference into two halves for the two five-phase VSIs, where the reference of the right inverter of Fig. 2 requires change of phase by 180 degrees due to the negative sign in (6). This will however only produce operation of the dual-inverter system that is identical in terms of performance to the single-sided two-level inverter supply.

The development of space vector PWM for the dual-inverter supply is therefore postponed for further work. Instead, operation is in what follows studied for the carrier-based PWM with reference splitting into two halves.

VI. Carrier-Based PWM

The applied carrier-based PWM is sinusoidal PWM with the triangular zero-sequence injection. As shown in [19], this carrier method is a full equivalent of the space vector PWM. The reference sinusoidal modulating signals are split into two halves and the reference voltages are phase-shifted by 180 degrees for the right-hand side inverter of Fig. 2. Dc link voltage of each inverter is set to 300 V (600 V single-sided supply mode equivalent), reference frequency is 50 Hz and the switching frequency of the two VSIs is 1 kHz. Two cases are investigated. In the first one the carriers of the two inverters are also phase-shifted by 180 degrees. In the second case the carriers are kept in phase.

The resultant operation of the dual-inverter system is in both cases equivalent, from the point of view of the number of levels in the phase voltage, to the single-sided supply with 600 V dc link voltage. However, the properties of the two strategies are quite different. Fig. 6 illustrates phase voltage and its spectrum for operation near the limit of the linear modulation region, with the total modulation index (defined as $V_{1peak}/(0.5V_{dc})$) of 1.05.

As can be seen from Fig. 6, phase voltage in both cases has nine levels, as the case is with the single-sided two-level VSI supply. However, the levels that appear in the phase voltage are different. In the case of 180° shifted carriers, the levels are the same as with a single two-level supply and correspond to $\pm(1/5)pV_{dc}$, where p = 0,1,2,3,4 (V_{dc} = 600 V). If carriers are kept in phase the phase voltage levels are $\pm(1/10)qV_{dc}$, where q = 0,1,4,5,6. Increments of 60 V correspond to the single-sided operation with a three-level NPC inverter for which, however, q would be taking all values from 0 to 8.

Hence only some of the possible levels are realised. It can also be observed from Fig. 6 that, if carriers are in phase, switching harmonics around the odd multiples of the switching frequency are cancelled out, so that the spectrum contains only harmonics around even multiples of the switching frequency. This effectively means that the overall system behaves as though switching frequency is 2 kHz rather than 1 kHz. This is beneficial since it would lead to a reduction of the current ripple.

The same study has been repeated for other modulation index values and the same behaviour has been observed with regard to both the level properties and the spectral behaviour.

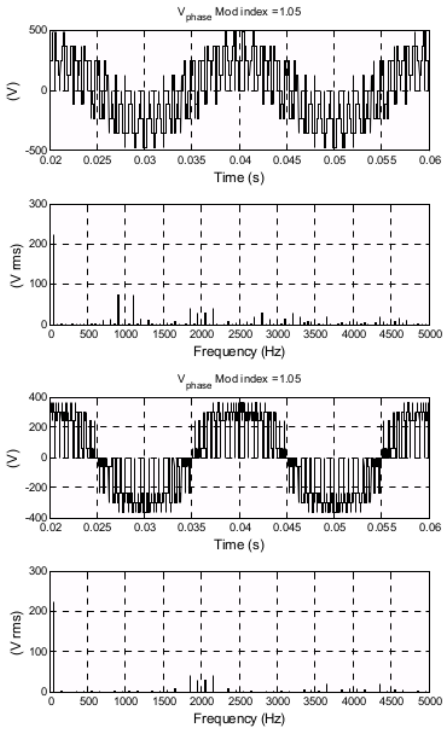

Fig. 6. Carrier-based PWM with triangular zero-sequence injection. Voltage reference split into two halves and carrier signals of the two inverters phase-shifted by 180° (top) and kept in phase (bottom).

VII. Conclusion

Dual-inverter supply properties for multiphase machines are investigated. Switching states for various phase numbers are discussed. Detailed analysis is performed for the five-phase case and all active phase voltage space vectors are determined. The total number of space vectors is 211, i.e. the same as with a three-level five-phase inverter supply in single-sided mode. However, the number of switching states is considerably higher (1024 versus 243) meaning that there is a considerably higher switching state redundancy.

Approaches to PWM control are further discussed, including space vector and carrier based methods. Some preliminary simulation results are finally reported for the carrier based PWM with triangular zero-sequence signal injection. The dual-inverter supplied multiphase machines are believed to hold a good prospect for potential utilisation in both EVs and HEVs.

References

[1] H. Stemmler, P. Guggenbach, "Configurations of high-power voltage source inverter drives," in *Proc. European Power Electronics and Applications Conf. EPE,* Brighton, UK, 1993, vol. 5, pp. 7-14.

[2] H. Stemmler, "High-power industrial drives," *Proceedings of the IEEE,* vol. 82, no. 8, 1994, pp. 1266-1286.

[3] D. Casadei, G. Grandi, A. Lega, C. Rossi, L. Zarri, "Switching technique for dual-two level inverter supplied by two separate sources," in *Proc. IEEE Applied Power Elec. Conf. APEC,* Anaheim, CA, 2007, pp. 1522-1528.

[4] C. Rossi, G. Grandi, P. Corbelli, D. Casadei, "Generation system for series hybrid powertrain based on dual two-level inverter," in *Proc. European Power Electronics and Applications Conf. EPE,* Barcelona, Spain, 2009, CD-ROM.

[5] C. Rossi, G. Grandi, P. Corbelli, "Series hybrid powertrain based on the dual two-level inverter,", in *Proc. Optimization of Electrical and Electronic Equipment OPTIM,* Brasov, Romania, 2008, pp. 277-286.

[6] D. Casadei, G. Grandi, A. Lega, C. Rossi, "Multilevel operation and input power balancing for a dual two-level inverter with insulated dc sources," *IEEE Trans. on Industry Applications,* vol. 44, no. 6, 2008, pp. 1815-1824.

[7] X. Kou, K. A. Corzine, M. W. Wielebski, "Overdistension operation of cascaded multi-level inverters," *IEEE Trans. on Industry Applications,* vol. 42, no. 3, 2006, pp. 817-824.

[8] Y. Kawabata, M. Nasu, T. Nomoto, E. C. Ejiogu, T. Kawabata, "High-efficiency and low acoustic noise drive system using open-winding AC motor and two space-vector-modulated inverters," *IEEE Trans. on Industrial Electronics,* vol. 49, no. 4, 2002, pp. 783-789.

[9] S. Lu, K. A. Corzine, "Advanced control and analysis of cascaded multi-level converters based on P-Q compensation," *IEEE Trans. on Power Electronics,* vol. 22, no. 4, 2007, pp. 1242-1252.

[10] G. Mondal, K. Sivakumar, R. Ramchand, K. Gopakumar, E. Levi, "A dual-seven-level inverter supply for an open-end winding induction motor drive," *IEEE Trans. on Industrial Electronics*, vol. 56, no. 5, 2009, pp. 1665-1673.

[11] E. Levi, "Multiphase electric machines for variable-speed applications," *IEEE Trans. on Industrial Electronics*, vol. 55, no. 5, 2008, pp. 1893-1909.

[12] O. Lopez, J. Alvarez, J. D. Gandoy, F. D. Freijedo, "Multi-level multiphase space vector PWM algorithm," *IEEE Trans. on Industrial Electronics*, vol. 55, no. 5, 2008, pp. 1933-1942.

[13] O. Lopez, J. Alvarez, J. D. Gandoy, F. D. Freijedo, "Multilevel multiphase space vector PWM algorithm with switching state redundancy," *IEEE Trans. on Industrial Electronics,* vol. 56, no. 3, 2009, pp. 792- 804.

[14] K. K. Mohapatra, K. Gopakumar, "A novel split phase induction motor drive without harmonic filters and with linear voltage control for the full modulation range," *EPE Journal,* vol. 16, no. 4, 2006, pp. 20-28.

[15] J. P. Martin, E. Semail, S. Pierfederici, A. Bouscayrol, F. Meibody-Tabar, B. Davat, "Space vector control of 5-phase PMSM supplied by 5 H-bridge VSIs," in *Proc. ElectrIMACS,* Montreal, Canada, 2002, CD-ROM.

[16] O. Lopez, E. Levi, F. Freijedo, J. D. Gandoy, "Number of switching state vectors and space vectors in multilevel multiphase converters," *Electronics Letters*, vol. 45, no. 10, 2009, pp. 524-525.

[17] A. Iqbal, E. Levi, "Space vector PWM techniques for sinusoidal output voltage generation with a five-phase voltage source inverter," *Electric Power Components and Systems,* vol. 34, no. 2, 2006, pp. 119-140.

[18] D. Dujic, M. Jones, E. Levi, "Generalized space vector PWM for sinusoidal output voltage generation with multiphase voltage source inverters," *Int. J. Industrial Electronics and Drives,* vol. 1, no. 1, 2009, pp. 1-13.

[19] D. Dujic, M. Jones, E. Levi, "Continuous carrier-based vs. space vector PWM for five-phase VSI," in *Proc. IEEE EUROCON 2007: Int. Conf. on 'Computer as a Tool'*, Warsaw, Poland, 2007, pp. 1772-1779.

A Multiphase Dual-Inverter Supplied Drive Structure for Electric and Hybrid Electric Vehicles(IEEEVPPC2010)

ORIGINALITY REPORT

19%	10%	19%	1%
SIMILARITY INDEX	INTERNET SOURCES	PUBLICATIONS	STUDENT PAPERS

MATCH ALL SOURCES (ONLY SELECTED SOURCE PRINTED)

4%

★ N. Bodo, M. Jones, E. Levi. "A PWM method for seven- and nine-phase open-end winding motor drives", Mathematics and Computers in Simulation, 2013

Publication

Exclude quotes	On	Exclude matches	< 1%
Exclude bibliography	On		

A Multiphase Dual-Inverter Supplied Drive Structure for Electric and Hybrid Electric Vehicles(IEEEVPPC2010)

GRADEMARK REPORT

FINAL GRADE

/0

GENERAL COMMENTS

Instructor

PAGE 1

PAGE 2

PAGE 3

PAGE 4

PAGE 5

PAGE 6

PAGE 7